

On the topology of a cyclic universe with colour fields

V. N. Yershov

Mullard Space Science Laboratory (University College London),

Holmbury St.Mary, Dorking RH5 6NT, UK

vny@mssl.ucl.ac.uk

Abstract

The topology of the universe is discussed in relation to the singularity problem. We explore the possibility that the initial state of the universe might have had a structure with 3-Klein bottle topology, which would lead to a model of an oscillating (cyclic) universe with a well-defined boundary condition having no singularity. The same topology is assumed to be intrinsic to the nature of the proposed primitive constituents of matter (colour preons) which gives rise to the observed variety of elementary particles. Some phenomenological implications of this approach are also discussed. PACS: 02.40.-k, 04.20.Dw, 11.15.Kc, 11.30.Na, 12.10.Dm, 12.60.Rc, 98.80.Bp. *Keywords:* *cyclic universe; singularity; composite particles; preons; tripolar fields.*

1 Introduction

During the past few years the old idea of a cyclic universe [1] has regained new ground following a series of publications by Steinhardt and Turok [2] describing a model based on 10-dimensional colliding branes. This model surmounts the hurdles of the previous cyclic-universe models, such as the problem of growing entropy and the lack of a realistic physical mechanism for the rebounding of the oscillating universe after each collapse. That is why the Steinhardt-Turok model has attracted much attention. However, it requires the universe to have at least ten spatial dimensions, which is not yet confirmed by observational evidence. Here we shall return to a three-dimensional cyclic-universe model, in which the distinction between matter and space is abandoned. That is, we shall regard the matter particles as stable configuration patterns of a moving manifold (space), as was proposed by Wheeler and others [3]. Representing space by a moving manifold is logical because one cannot actually deal with the notions of space and motion separately from each other, as the use of one of them requires invoking the other and vice versa. We shall focus mainly on the topological aspects of the problem, gaining insight into the nature of the cosmological singularity. We also expect this approach to shed light on the singularity problem related to microscopic and macroscopic objects, such as elementary particles and collapsed stars.

Astronomical observations provide strong evidence that compact objects with sufficiently large masses for complete contraction do exist in nature [4], e.g., in compact binary systems [5] with calculable masses of the components, in ultra-luminous compact X-ray sources [6] whose luminosities exceed the Eddington luminosity of a 100-solar-mass object, and in galactic nuclei [7] where the physical processes and the dynamics of stars near the nucleus indicate that the mass of the central object exceeds 10^8 to 10^9 solar masses. Such objects are routinely called supermassive blackholes. From the theoretical point of view, the centres of these objects must contain spatial singularities. Plausible evidence exists [8] that the universe in its past was also squeezed to a very small volume, which is regarded by the standard cosmological model as an indication that the universe was born from a singularity.

On the other hand, there is no physical evidence for spatial singularities whatsoever. So it would be logical to distinguish between the notions of “blackhole” and “singularity”. The former could be regarded as related to a real physical object compressed below its Schwarzschild radius [9], whereas a singularity, being a mathematical point, conflicts with physical reality. Based on scientific grounds, one can hardly accept the possibility of a physical object transforming into a mathematical abstraction (a point) and vice versa. The existence of singularities necessarily implies infinite gravity and, hence, the availability of an infinite amount of energy from finite sources. If a singularity is a point (in the mathematical sense) then the universe, born from a singularity, must have passed from non-existence to existence, which violates the conservation principle.

The idea of the point-like state of the universe was rejected by many physicists, proposing a variety of mechanisms to avoid it. Yet, the common belief is that general relativity based on idealisations, like any other theory, has a limited domain of validity, and that another theory (quantum gravity) has to be developed to deal with singularities [10]. Then the singularity must be “smeared” by quantum fluctuations [11]. But still there are some hints that this might not be the case: specially organised astronomical observations [12] detect no quantum fluctuations in vacuum which are needed to smear the singularity. It has also been indicated in the literature [13] that the effects of quantum gravity, which have had 10^{10} years to act on the gamma-ray burst photons, should completely randomise the polarisation of these photons, contrary to what is observed [14].

Following these clues, we shall explore here the possibility that general relativity is valid on all scales and that space is smooth down to arbitrarily small distances, containing no regions with infinite curvatures. In other words, we hypothesise that there should exist an upper bound to spacetime curvature, which is a natural assumption, given that sources of infinite energies are not observed in nature. A singularity then could be regarded as a topological feature of the manifold rather than its discontinuity.

One can consider such an object as a basic element of composite particle systems, developing the ideas of the preon-based composite models of elementary particles. In fact, considering topological features [15] or microscopic blackholes [16] as elementary particles is not new and is widely discussed in the literature. Here we shall look at this possibility from a slightly different point of view by assuming that topological features can form stable bound states related to the structure of elementary particles. We shall outline the proposed approach in the next two sections. Then, in Sections 4 and 5, we shall demonstrate the functionality of this model by presenting a few simple examples of preonic bound states. In Section 6 we shall comment on some possibilities of experimental verification of our model, and in Section 7 we shall discuss some implications of this approach in connection with the problems of cosmological singularity and the oscillating universe models.

2 Primitive particle

Consider a spinning 3-manifold (e.g. a sphere), $\mathcal{S} \in \{\mathbb{S}^3\}$, of radius $R_{\mathcal{S}} \in (-\infty, +\infty)$ formed of a massless elastic fluid – a collection of worldlines of test particles. The rotation of \mathcal{S} corresponds to a 4-velocity \mathbf{u} of the fluid in all possible directions through each point of the spatial slice of the manifold. Let the manifold be punctured, $\mathcal{S} \rightarrow \mathcal{S} \setminus \{0\}$, that is, containing a point-like dislocation σ , Fig.1, which can be regarded as a primitive particle (also called preon) having no properties except for the property of possessing a charge (inflow or outflow of test particles, as indicated by arrows in Fig.1).

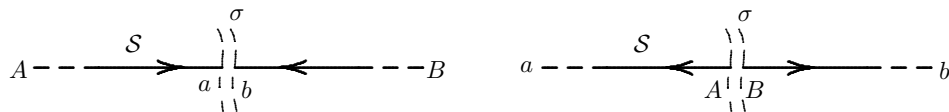


Fig. 1: A point-like topological feature σ on a (locally flat) 3-manifold \mathcal{S} with the boundaries of \mathcal{S} labelled as AB and ab . The inflow (left) or outflow (right) of test particles is regarded as a charge of σ .

Given a compact control surface \mathcal{C} on \mathcal{S} ($\mathcal{C} \in \mathbb{S}^2$) with no dislocations (singularities) in its interior, the inflow through this surface should be equal to the outflow (Fig.2), which is the usual flow conservation condition. In the case of a singularity σ enveloped by \mathcal{C} , either inflow or outflow vanishes, which is not consistent with the conservation principle. To restore consistency, the flow should be sent back to \mathcal{S} , which can be done through the boundaries by identifying ab with AB :

$$\begin{aligned} a &\rightarrow A \\ b &\rightarrow B \end{aligned} \tag{1}$$

or by crisscrossing them:

$$\begin{array}{ccc} a & A \\ \diagup \!\! \diagdown & & \\ b & B \end{array} \tag{2}$$

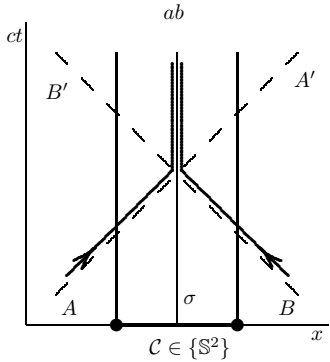


Fig. 2: Worldlines of flow particles AA' , BB' (no singularity) and Aa , Bb (entering a singularity σ wrapped with a control 2-sphere C). The latter violates the conservation principle.

The resulting shape is a hypertorus \mathbb{T}^3 (for the first case), or the Klein bottle \mathbb{K}^3 (for the case with the crisscrossed boundaries). This restores the integrity of the flow and avoids the discontinuity of the manifold at the point of singularity. The above identification of the boundaries implies the existence of closed causal curves, which could be viewed as a problem, though it is known that such curves are allowed to exist by general relativity, which is under intense debate in the literature [17]. In our case, the closed curves are self-causal, which avoids the related paradoxes. The inflow (outflow) Q through this object is still not accounted for, but the total flow of the system is conserved.

3 The field of the primitive particle

By regarding the described dislocations of the manifold as primitive particles we have to assume the possibility of these particles interacting with each other; i.e., exercising a force on each other, which in our case is realised by fluid pressure and tension. The corresponding field, φ , can be defined in terms of the flow density through an arbitrary 2-surface \mathcal{C} surrounding σ . This field is spherically symmetric and roughly inversely proportional to the squared distance between \mathcal{C} and σ . However, it is topologically impossible to enclose the central opening (σ) of a 3-torus with an arbitrary 2-surface. Due to this problem, the definition of φ in our case has to be modified. Let $\tilde{\mathcal{C}}$ be a 2-sphere of radius $R_{\tilde{\mathcal{C}}} \in (0, \infty)$ on $\mathcal{S} \in \{\mathbb{T}^3\}$ or $\{\mathbb{K}^3\}$ with its centre at σ (but not enveloping σ), as shown in Fig.3; namely, by sliding $\tilde{\mathcal{C}}$ along \mathcal{S} towards σ . The total flow \tilde{Q} through $\tilde{\mathcal{C}}$ is nil since σ is not enveloped by $\tilde{\mathcal{C}}$. However, σ divides $\tilde{\mathcal{C}}$ into

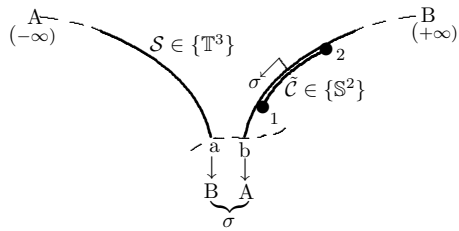


Fig. 3: The “throat” (topological feature) σ of a hypertorus \mathbb{T}^3 or the Klein bottle \mathbb{K}^3 and a control sphere $\tilde{\mathcal{C}} \in \mathbb{S}^2$ placed at σ by sliding $\tilde{\mathcal{C}}$ within \mathcal{S} towards the topological feature.

two hemispheres, so that the flow \tilde{Q} is split into two parts corresponding to the outermost and innermost hemispheres of $\tilde{\mathcal{C}}$. By calculating the flow density at the innermost “1” and outermost “2” points of $\tilde{\mathcal{C}}$ (Fig.3) one can resolve the field φ into two components:

$$\varphi(\rho) = \varphi_1(\rho) + \varphi_2(\rho). \quad (3)$$

Although the flow line density grows as $R_{\tilde{C}}$ decreases, this density will have a minimum at the origin (or will even vanish in the case of a non-compact manifold) since the boundary of the origin σ is identified here with the outer (larger) circumference of the torus, which is infinite in the case of a non-compact manifold. The corresponding boundary condition (for a non-compact manifold) will be

$$\varphi_1(0) = \varphi_2(0) = 0. \quad (4)$$

Then it follows that at some distance from σ the density of flow lines must have a maximum, which would supposedly correspond to the upper bound of the manifold's curvature. When changing $R_{\tilde{C}}$ (say, from zero to a maximal value), the points "1" and "2" of \tilde{C} take opposite paths on the manifold:

$$\begin{aligned} "1" : & A \rightarrow a \\ "2" : & a \rightarrow A \end{aligned} \quad (5)$$

which would result in an asymmetry between the two components of the field; namely, $\varphi_2(\rho)$ will grow from a minimum (zero) to some maximal value, then decaying again to a minimum at the end of the path of the point "2" (Fig. 4). The component $\varphi_1(\rho)$ will uniformly grow for most of the path of "1". Of course, eventually, at the end of this path φ_1 will decay to a minimum (zero). Then, the second boundary condition for a non-compact manifold will be

$$\varphi_1(\infty) = \varphi_2(\infty) = 0. \quad (6)$$

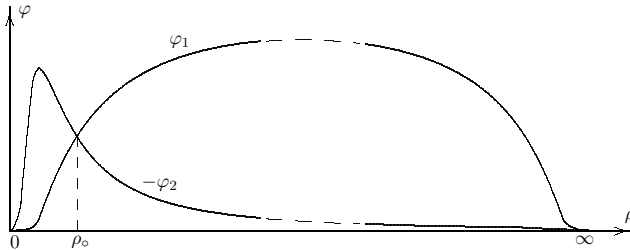


Fig. 4: Two components, φ_1 and φ_2 , of the equilibrium field corresponding to the innermost and outermost points of the control sphere \tilde{C} .

One should also take into account torsion which, in the case of a 3-manifold, has three degrees of freedom [18], and which would lead to the nonlinear Heisenberg equation [19] and nonabelian degrees of freedom. The corresponding field would have a topological quantum number – the colour analogy of helicity in fluid dynamics [20]. In the three-dimensional case there are six possible helical flow orientations, as distinct from, for instance, two-dimensional flow, with its bipolar vorticity and only four possible flow orientations [21]. Then, one can devise a force between primitive particles by regarding, for example, the vortex flow lines as electric currents [22] and calculating the Lorentz force between these currents. It follows that in the case of two like-charged (say, with inflows) primitive particles of opposite vorticities the force φ_1 between the flow lines is attractive and φ_2 is repulsive. If the particles have like-vorticities the force φ_1 will be repulsive.

This accords with the known pattern of attraction and repulsion between colour charges [23]: two like-charged but unlike-coloured particles are attracted, otherwise they repel. We can see that the colour pattern is readily understood in terms of flow vortices on a manifold with the T^3 or K^3 topology. The approximate antisymmetry of φ_1 and φ_2 in the vicinity of the origin implies that there should exist an equilibrium distance, $\rho_0 > 0$, such that

$$\varphi_1(\rho_0) = -\varphi_2(\rho_0), \quad (7)$$

in which case the fields cancel each other. This breaks the initial spherical symmetry of the field, as well as the symmetry of scale invariance, and allows structure formation in the framework of this model.

4 The simplest bound states of colour preons

Let us consider some simple structures based on the fields (3) with the boundary conditions (4) and (6) and the equilibrium condition (7). The following functional form for the components of this field:

$$\begin{aligned}\varphi_1(\rho) &= \varkappa \exp(-\kappa\rho^{-1}) \\ \varphi_2(\rho) &= -\varphi'_1(\rho)\end{aligned}\quad (8)$$

satisfies the conditions (4) and (7). It does not match the second boundary condition (6) but this does not matter for the cases with typical distances between particles of the order of a few units of ρ_0 . The basic field does not necessarily have to be of the simplest form (8). Its main feature (the capability of generating equilibrium particle configurations) could be derived from various physical considerations, including the geometry and shape of the manifold, as was shown in [24]. It is also possible to satisfy the boundary condition (6) by modifying the first component of the field in such a way as to nullify it at infinity, e.g.,

$$\tilde{\varphi}_1(\rho) = \rho^{-1} \varphi_1(\rho). \quad (9)$$

Nevertheless, for short distances we can adopt the field (8) as a simple example to illustrate the functionality of our model. This field corresponds to the following double-well potential:

$$V(\rho) = (1 - \rho) \exp(-\kappa\rho^{-1}) - \text{Ei}(-\kappa\rho^{-1}). \quad (10)$$

For simplicity the range coefficient κ can be set to unity. The coefficient $\varkappa = \pm 1$ in (8) denotes the polarity of the field and must be chosen such as to reproduce the above pattern of long-range attraction and short-range repulsion between particles.

A field of this kind reveals a potential surface with multiple local minima leading to kinematic constraints of a topological nature, which is analogous to the cluster formation scheme in molecular dynamics [25]. The only difference is that here we have to deal with the tripolarity of the fields. These topological constraints determine a unique set of clusters, the simplest of which are colour dipoles and tripoles composed of, respectively, two and three preons. Obviously, the dipoles are deficient in one colour, whereas the tripole fields are colourless at infinity and colour-polarised nearby, which allows axial (pole-to-pole) coupling of these structures into strings.

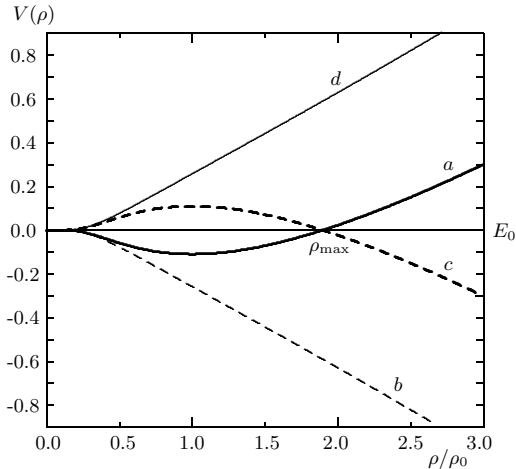


Fig. 5: Equilibrium potential $V(\rho)$ corresponding to a colour-dipole system; (a) two like-charged particles with unlike colours; (b) the same but with like-coloured particles; (c) oppositely charged particles with like colours; and (d) oppositely charged particles with unlike colours.

The potential (10) is graphically shown in Fig. 5 *a*. This is a typical double-well potential, which is known to lead to chaotic oscillations and stochastic resonances [26]. It is also known to be self-calibrated; i.e., it establishes the length, time and energy scales by, respectively, the separation between wells, oscillation frequency in the inverted barrier and barrier height. We shall use the half-separation between

wells (the equilibrium distance, ρ_o , corresponding to the minimum of the potential) as the basic unit length for this model. The speed unit, v_o , is also intrinsic to the potential (10) in the sense that, given the initial energy, E_0 , one can calculate the corresponding speed of a particle moving in this potential. For example, the speed of a two-preon system with the potential (10) is calculated as

$$v(\rho) = \sqrt{2(E_0 - V(\rho))/\hat{m}}, \quad (11)$$

where $\hat{m}^{-1} = m_1^{-1} + m_2^{-1} = \frac{1}{2}$ is the reduced mass. By setting the energy E_0 to some level, say, to zero at $\rho = \rho_{\max}$ we can calculate the maximal speed, $v_{\max} = v(\rho_o) \approx 0.937v_o$, expressed in units defined by the amplitude and range coefficients of the function (8). This also establishes the time scale by defining a unit time interval, t_o , such that $v_o t_o = \rho_o$, as well as the other necessary units, like, e.g., the unit of angular momentum, L_o , which would correspond to a preon of unit mass, m_o , moving with unit speed, v_o , along a circular path with unit radius, ρ_o . The mass unit, m_o , can be defined by calculating the energy of the field φ for a single preon:

$$m^2 = \frac{1}{2\pi} \int_S \varphi^2 dS = 1 \quad (12)$$

with the first component of the field, φ_1 , removed because the integral $\int \varphi_1^2 dS$ diverges and, obviously, cannot be used for this purpose. If we ignore for a moment the third colour and consider a two-body system

$$d_y^+ = \sigma_r^+ \wr \sigma_g^+ \quad (13)$$

– a charged colour dipole with energy $E_0 = 0$ – we can see that the charges in this system are confined (oscillating) within the region $(0, \rho_{\max})$, where $\rho_{\max} \simeq 1.894\rho_o$ (see Fig. 5). The symbol \wr between σ_r^+ and σ_g^+ in (13) simply indicates that these two components oscillate with respect to each other; and the index “y” (yellow=blue) indicates that this structure is deficient in the blue-polarity field, φ_1^b , which means that the charged colour dipole d_y^+ cannot actually exist in free states by having infinite energy (unless we neglect the third colour). The net charge of d_y^+ corresponds to $+2q_o$. Its mass, $m_{d_y^+}$, in the first approximation, is equal to $2m_o$, which is the exact value for the case when the centres of σ_r^+ and σ_g^+ coincide and the components φ_1^r and φ_1^g of the field cancel each other exactly (the component φ_1^b being ignored).

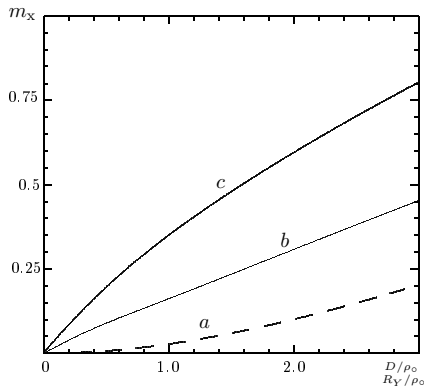


Fig. 6: Mass excess (in units of m_o) for some simple preon systems (normalised to the number of preons in the system) as a function of distance D between preons. (a): A system of two like-charged preons with unlike colours; (b): two unlike-charged preons with unlike colours, and (c): three like-charged preons with unlike colours (in this case the abscissa corresponds to the tripole radius, R_Y).

If the constituents of d_y^+ are separated by some distance, D , the fields φ_1^r and φ_1^g will cancel only partially and the mass of this system will exceed the value $2m_o$ by a quantity (called hereafter the mass excess) which can be calculated by using (12). The mass excess of the two-component system d_y^+ as a function of distance between the components is shown in Fig. 6a. In its ground state ($D = \rho_o$) this system has a mass of $\approx 2.04 m_o$.

For the system of two preons with like colours, say $\sigma_r^+ \sigma_r^+$, we have to reverse the sign of \varkappa in (8), which would result in a repulsive combined potential (curve *b* in Fig. 5) having a maximum at the origin. This means that the system $\sigma_r^+ \sigma_r^+$ cannot be formed in principle, even by neglecting the third colour.

The wells of the potentials corresponding to the preon pairs with opposite electric charges (curves *c* and *d* in Fig. 5) imply that the neutral colour dipoles

$$d_y^0 = \sigma_r^+ \wr \sigma_g^- \quad \text{and} \quad d_r^0 = \sigma_r^+ \wr \sigma_r^- \quad (14)$$

could, in principle, be formed if the third colour were neglected. Then, the system d_y^0 would have a vanishing mass (100% mass defect) for $D = 0$ because in this case not only do the fields φ_1 of its two constituents have opposite signs and cancel each other, but the fields φ_2 also do. For $D > 0$ the mass of d_y^0 will be growing almost linearly with distance, as shown in Fig. 6*b*.

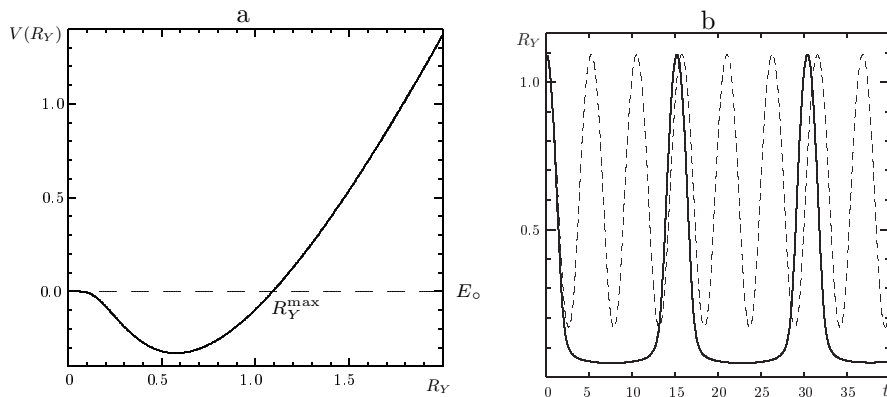


Fig. 7: (a) Potential energy of the tripole system Y as a function of its radius R_Y ; (b) The pattern of radial oscillations of a tripole with invariable mass (solid curve), and with the mass excess function taken into account (dashed curve). The amplitude of the oscillating R_Y corresponds to the energy level $E_0 = 0$. Here time is in units of t_o and the radii are in units of ρ_o .

The colourless bound state of three like-charged preons with complementary colours (the tripole)

$$Y^+ = \sigma_r^+ \wr \sigma_g^+ \wr \sigma_b^+ \quad \text{or} \quad Y^- = \sigma_r^- \wr \sigma_g^- \wr \sigma_b^-, \quad (15)$$

has a finite mass. Given $E_0 = 0$, the tripole's radius, R_Y , will oscillate between zero and $R_Y^{\max} \simeq 1.09\rho_o$, see Fig. 7. The tripole system must be stable because it would take an infinite amount of energy to remove any of its three constituents from the system. In their ground state, these constituents will be separated from each other by the distance $D = \rho_o$, corresponding to the tripole's equilibrium radius, $R_Y = \rho_o/\sqrt{3}$, which minimises the potential shown in Fig. 7. Since the centres of the tripole constituents do not coincide, the fields φ_1 are cancelled only partially and the mass of the tripole's ground state has an excess of about $0.199 m_o$ per preon over the mass of the state with $R_Y = 0$ (curve *c* in Fig. 6).

5 Two- and three-component strings of tripoles

Due to colour-polarisation of the tripole's fields, different tripole can interact with each other and form bound states. The simplest of them is a two-component string formed of either two like-charged tripole:

$$\gamma^+ = Y^+ \wr Y^+ \quad \text{or} \quad \gamma^- = Y^- \wr Y^-, \quad (16)$$

or oppositely charged tripole:

$$\gamma^\circ = Y^+ \wr Y^-. \quad (17)$$

Obviously, the tripole in these systems will be joined pole-to-pole to each other, rotated by 180° (see the scheme on the left of Fig. 8). The corresponding potential energies for the pairs of like- and unlike-charged tripole as functions of tripole's radii, R_Y , and separation, D , between the tripole are shown in Fig. 8 (a) and (b), respectively.

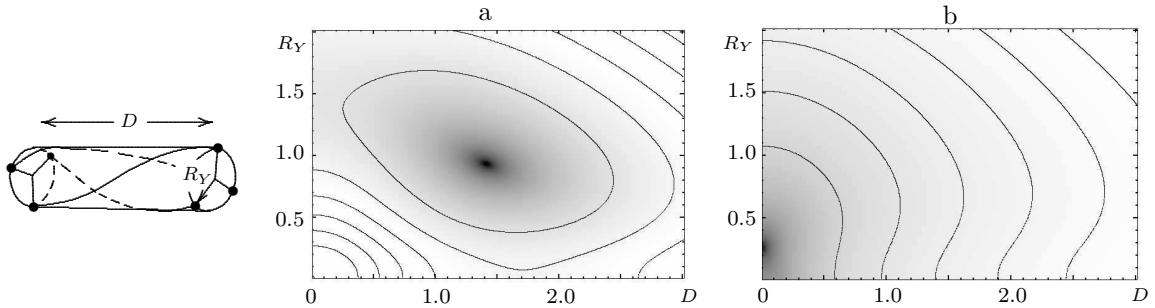


Fig. 8: Potential energy of a string formed of two tripole Y separated by distance D and having radii R_Y (scheme on the left); (a) two like-charged tripole; (b) two oppositely charged tripole.

The minimum of the potential for the second (electrically neutral) system γ° , Fig. 8 (b), is very close to the origin, which means that both electric and colour fields in this system (particle) are cancelled almost entirely. Therefore, in its ground state this particle will have a vanishing mass and will not be able to interact with other similar (neutral) particles, so that in each point of the manifold one can place as many of them as one pleases (the density of the population is not derivable from first principles). By being massless, these particles will move with maximal available speed in all possible directions through each point of the manifold, which can be regarded as an ideal gas of neutral particles. However, in the vicinity of an electric or colour charge the constituents of γ° will be polarised either electrically or chromatically, converting this particle to an electric or colour dipole. This property of γ° is important because within this framework one can use the gas of these particles to represent a polarisable medium (vacuum) where the motions and interactions of all other particles take place. The dipole-dipole interactions between the polarised γ° -particles will result in the formation of instantaneous preonic configurations of different complexity, which can be regarded as a source of new particles, provided the supplied energy is sufficient for the complete separation of the polarised components of γ° (otherwise, these configurations could be used for modelling virtual particles).

By analogy with the three-component system (15) we can consider a three-component string, e^\pm , formed of like-charged tripole:

$$e^+ = Y^+ \wr Y^+ \wr Y^+ \quad \text{or} \quad e^- = Y^- \wr Y^- \wr Y^- . \quad (18)$$

The potential energy of this string will be minimised for its loop-closed configuration with its constituent tripole rotated by 120° with respect to each other (see the scheme on the left of Fig. 9). The minimum of the potential surface shown in Fig. 9 corresponds to the static equilibrium of this loop.

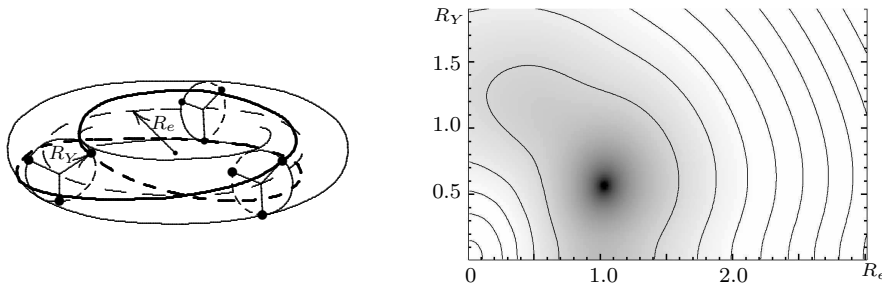


Fig. 9: Potential surface corresponding to the loop e^\pm of radius R_e formed of three like-charged tripole Y with radii R_Y (scheme on the left). The radii are expressed in units of ρ_0 .

In reality, such a static state cannot be stable because the tripole comprising the loop retain their rotational and translational degrees of freedom (around and along their common ring-closed axis) and will be moving under the influence of all the other existing particles, for example, under the stochastic action of the above mentioned gas of the neutral two-component tripole strings. The dynamical parameters of this system will be quite different from those corresponding to the static case shown in Fig. 9 because each of the spinning tripole will generate a magnetic field modifying (and stabilising) the motions of the two other tripole in the loop. By the standard dynamo mechanism these motions will induce toroidal

and poloidal magnetic fields which in turn will maintain the rotational and orbital motions of the looped tripoles. (We shall discuss the dynamics of this system elsewhere.)

The colour-currents corresponding to the motion of each individual preon in this system are helices (Smale-Williams curves) which, by their closure, make a π -twist around the ring-closed axis of the structure with either clockwise or anticlockwise winding (the scheme shown in Fig.9 corresponds to the anticlockwise winding of the currents). Such a twisting dislocation of the phase is a conserved quantity called topological charge [27] or dislocation index, which has a sign corresponding to the winding direction (clockwise or anticlockwise) and the magnitude related to the winding number per 2π -orbit path. In these terms, the π -phase shift of the currents in the structure e^\pm corresponds to a topological charge $S = \pm \frac{1}{2}$, identifiable also with the particle internal angular momentum (spin).

The path of each preon belonging to a particular dipole overlaps exactly with the paths of two other preons that belong to two other tripoles of the structure and whose colour charges are complementary to the colour charge of the first preon. That is, the currents that form the structure e^\pm are dynamically colourless and, averaged in time, the field of this particle will have only two polarities corresponding to the conventional electric field.

6 A hierarchy of preonic bound states

One finds that, besides the simplest bound states of colour preons discussed in the previous sections, the field (8) gives rise to a rich variety of other structures. For example, a string of dipole-antidipole pairs has a symmetry similar to that of the structure (18), which allows its closure in a (minimal) loop, ν_e , containing six such pairs (twelve tripoles). Like e^\pm , this structure is also dynamically colourless but, unlike e^\pm , it is electrically neutral. Despite its null electric and colour charges, the particle ν_e can, nevertheless, interact with e^\pm through its residual chromoelectric fields, given that the motions of the constituents in both structures are synchronised. In fact, the synchronisation of processes in neighbouring structures is a universal property of nature [28], so that the structures ν_e and e^\pm will, indeed, interact with each other, the more so because, curiously enough, the helical patterns of their colour currents perfectly match each other, as a screw and its nut, provided that the two particles have like-topological charges (spins), otherwise their residual chromoelectric fields will be repulsive. Two like-topological charges attract each other only if the particles carrying these charges were of two different kinds with the distinct radii of their loops, allowing one of them passing through the central opening of the other (which is the case for the structures ν_e and e^\pm). Particles of the same kind and size (e.g., two particles e^\pm) will be repulsed from each other by having like-topological charges and attracted to each other by having opposite topological charges. This feature of the dipole loops might shed some light on the origin of the Pauli exclusion principle.

By their properties (which include spin, charge, gyromagnetic ratio and parity) the three- and twelve-dipole loops (e^\pm and ν_e) can be identified with the electron and its neutrino, respectively. It can be seen that different combinations of these loops (involving also the tripoles Y^\pm) constitute a hierarchy of structures identifiable with the observed variety of elementary particles [29], including their known bound states and resonances, like mesons and baryons. Due to the topological constraints, the number of constituents in each structure is well-defined by the minimum of its potential energy, so that the hierarchy turns out to be unique.

The masses of these structures ensue from the energies of the motions of their constituents less binding energies (mass defects), which are known as standard mass-generating mechanisms for the composite systems. Therefore, within the framework of this model, there is no need of extra fields, like Higgs, to generate particle masses. In fact, this means that our model favours the negation of the existence of the Higgs' particle and predicts that it will never be found. The same null prediction can be made with respect to the supersymmetric partners of the known particles, since this model does not generate more structures than are needed to explain the origin of the observed variety of particles.

The fields of opposite polarities (or complementary colours) almost entirely cancel each other if two unlike-charged particles (structures) overlap or get close to each other, which also nullifies the masses of the neutral loops, like ν_e . This accounts for the so-called "mass paradox", according to which the momentum uncertainty for the constituents of a structure confined in a small volume of a composite particle should necessarily be greater than the mass of the host particle they comprise. In our case the almost infinite energies of the primitive particles are nullified by their binding energies, as in many composite models [30].

As was estimated in [31], the radius of the toroidal structure corresponding to the composite electron is $R_e \approx 15R_Y$. If we take a rather conservative estimate of the electron radius, $R_e = 10^{-22}$ m, based on the extrapolation of the g -factor to radius ratio for the known near-Dirac particles [32], then the corresponding binding energy between the dipoles constituting the composite electron would be $\sim 10^4$ TeV, which is far greater than the energy scales accessible by modern experimental techniques. For example, the proton beam energy of CERN's Large Hadron Collider (LHC) is expected to be of about 7 TeV [33]. Thus, according to our model, there must be a huge gap between the physics described by the standard model and the underlying level of physical reality. This would likely result in very few (if any) new phenomena observable with the use of the most powerful modern colliders.

Nevertheless, it is quite possible that some phenomena, either supporting or falsifying our model, could be seen at the TeV energy scale. For instance, quark sub-structures might be revealed by the LHC in the form of deviations from the QCD expectation of the high energy part of the jet cross-sections [34] and also in hadronic di-jets angular correlations [35].

As was mentioned in Section 3, our model is based solely on the symmetry $SU(3) \times U(1)$ of the basic field, whereas the weak interaction is viewed as a low-energy property of composite systems. That is, the weak interaction in our model is not fundamental but a residual effect of underlying chromoelectric fields, similar to the Yukawa interaction between nucleons, which is thought to be a residual interaction between quarks inside each individual nucleon. This is a situation typical for most composite models [36]. It is worth mentioning also that excluding the weak force from the fundamental forces is not at all unreasonable from a theoretical point of view and does not create any problem in the rest of physics, as was recently shown by Harnik, Kribs and Perez [37]. It follows that the weak gauge bosons should also be composite, exhibiting highly nonlinear oscillations of their sub-components [29]. When interacting with each other, the weak gauge bosons would induce synchronous motions of their sub-components, forming chains of coupled oscillators, which might be observable in the TeV energy range within the reach of the LHC.

The composite nature of particles, e.g. of the electron, might also reveal itself at low energies through synchronisation between the constituents of the composite electrons in ferromagnetic electron liquids [38] and low-dimensional electron systems, like Wigner crystals [39]. Another possibility is to detect some exotic electron bound states, like those observed by Jain and Singh [40] in their experiments at CERN aimed at searching for low-mass neutral particles decaying into e^+e^- pairs. They have reported the detection of short-lived neutral particles having masses of 7 ± 1 MeV and 19 ± 1 MeV. The former might correspond to the minimal spherically closed shell of eight electron-positron pairs [29] comprising a mass of about 8 MeV, less, of course, the binding energy between the constituents of this shell.

7 Cosmological singularity

The preonic structures discussed in the previous sections correspond to large manifolds, whereas for a reduced volume the situation must be quite different. Let us assume that our manifold \mathcal{S} is evolving (either expanding or contracting), with its curvature changing in time. It is not unreasonable to suppose that the coefficient κ in (8) establishing a natural upper bound on space curvature remains constant (given the strong observational constraints on the variability of particle properties [41]). This might shed light on some important cosmological problems.

Entropy problem. During the contraction phase (in an oscillating universe) the growing curvature of the manifold will reach a value comparable to the intrinsic curvature of the primitive particles. Since the potential (10) has a stationary point at the origin, all the primitive particles on \mathcal{S} will be squeezed into a minimal volume, their centres coinciding in the origin.

At this stage the contraction rate and the curvature of the manifold are maximal, whereas its volume is minimal (but not vanishing). Obviously, the minimised volume of the system precludes any structure formation because the superimposed primitive particles lose any degree of freedom for motion. Therefore, the entropy of the collapsed system is minimised, as opposed to the conventional view that entropy never decreases [42]. This simply reflects the fact that entropy, being a macroscopic statistical parameter, cannot be used for characterisation of a single-element system like the collapsed universe modelled with the fields (8).

Topological problem. The dynamics of the collapsing universe necessarily requires its further evolution (expansion). One can notice that a hypersphere \mathbb{S}^3 or the hypertorus \mathbb{T}^3 cannot pass from the contraction to expansion phase without reversing the direction of motion, which is impossible when the

contraction/expansion rate is maximal. This leaves us with only one possibility: the universe's topology must be \mathbb{K}^3 , which is the topology that allows passing from the contraction to expansion phase with maximal speed and without reversing the direction of motion.

Flatness problem. \mathbb{K}^3 is known to belong to the class of Euclidean manifolds, which are finite and geodesically complete [43], implying that any metric on a Klein bottle is conformally equivalent to a flat metric [44]. Moreover, in our case the global geometry of the universe should be very close to Euclidean at any stage of its evolution. This can be seen simply from the fact that in the \mathbb{K}^3 case the manifold is turned “inside-out”, with the curvatures of the “inner” and “outer” parts of the manifold being equal by their magnitudes and opposite in sign. The total curvature would then be observed almost vanishing, with a residual effect due to the presence of matter (primitive particles), so that our model implies a nearly flat universe, which is what is actually observed [45].

Charge asymmetry. The model described is symmetric with respect to the number of positive and negative charges (right and left parts of Fig.1) as each such pair is viewed as a manifestation of the same topological feature. However, it is known [46] that spacetime manifolds with nontrivial topology, like, e.g., $\mathbb{R}^3 \times \mathbb{S}^1$ or $\mathbb{R} \times \mathbb{T}^3$, can result in breaking of Lorentz and CPT invariance. In simple terms, the charge asymmetry within the framework of the colour preon model could be understood in terms of the distinct paths that inflows and outflows of test particles take on the “inner” and “outer” sections of the manifold. This is likely to lead to a difference in the energy content of these two sections because, due to the existence of an upper limit on the manifold's curvature, these sections will never overlap exactly and, thus, will have slightly different volumes, except for the instantaneous configuration corresponding to the maximal contraction phase. The sign of the difference between their energies will be reversed after each recollapse of the manifold, recovering the CPT symmetry for the entire expansion-contraction cycle.

Horizon problem. So far we have assumed that the magnitude of the fundamental speed, \mathbf{u} , (see Section 2) is constant. However, the conservation of angular momentum requires this speed to vary when the radius of the spinning manifold \mathcal{S} changes; it should have been maximal when the universe was passing from the contraction to expansion phase and zero when the universe reaches its maximal size. A series of models was developed [47], assuming the variability of the fundamental speed, in order to resolve the horizon problem and explain the relative smallness of the cosmological constant at present [49], without focusing specifically on the possible mechanism of this variability. In our case the variability of the fundamental speed necessarily follows from the conservation principle, providing an alternative to the standard inflationary picture and leading to predictions with respect to the homogeneity, flatness and perturbation spectrum, agreeing with observations in the same way as the predictions made by the standard inflationary model [48]. So, the colour-preon model fully embraces the variable fundamental speed theory with its broad field for future theoretical and experimental research.

Structure formation. The potential (10), by having an unstable stationary point at the origin, implies spontaneous symmetry breaking, resulting in self-organisation of colour charges in complicated structures from the very beginning of the manifold expansion. A system of primitive particles confined within a small volume will undergo a series of phase transitions when this volume changes. The initial spherical symmetry of the field and the symmetry of scale invariance will be broken when the size of the universe grows to a few units of ρ_0 . The further growth of the volume of the universe implies formation of a complicated network of tripole strings and loops, similar to the carbon nanotubes and fullerenes, as was shown in [29]. It is likely that the subsequent large-scale structure formation in the universe would have been affected by these initial tripole-based structures.

Dark energy. Besides the repulsive and attractive forces due to the $SU(3) \times U(1)$ symmetry of the basic field of this model, there should exist a force due to the local gradients of the curvature in the vicinity of each primitive particle. Since the gradient of the curvature is spherically symmetric around the origin, the corresponding reaction force (pressure P) is centripetal and spherically symmetric. Thus, in the reference frame of σ_i the primitive particle σ_j will experience a differential pressure directed towards σ_i and vice versa, so that the particles in the pair will be accelerated towards each other if no other forces counteract this pressure. In addition to the pressure P there should exist a global pressure [50], say p , positive, negative, or zero, depending on the sign of the residual curvature of the manifold (see above), which could give rise to a non-vanishing cosmological constant / dark energy [51]. Obviously, $|p| \ll |P|$ because the local curvature (corresponding to the pressure P in the vicinity of the primitive particle) is very large.

8 Conclusions

As we have seen, the framework outlined here appears to be no less natural than the standard inflationary model. The problems with entropy, horizon and flatness of the universe can be addressed without invoking entities of an unknown nature, like inflaton fields or extra dimensions. The cosmological singularity is in our case avoided by assuming some degree of rigidity of the manifold (which also gives rise to the hierarchy of elementary particles). According to this model, the observed characteristics of the universe emerge as a result of phase transitions in the early universe, corresponding to different structural levels of matter on the sub-quark scale. Given the enormous energies implied for the bonds between the clustered sub-quark particles, one should expect similar phase transitions and degeneracy states to occur during the collapse of a stellar object (of course, in the reverse order). The corresponding forces would be increasing from state to state downwards, counter-balancing gravity and preventing this object from complete collapse, even in the case of a supermassive blackhole.

Two of such degeneracy states (white dwarfs and neutron stars) are commonly known; two others – such as quark and preon stars – are hypothesised. Our model predicts that some other compact “dark objects” corresponding to the lowest structural levels of matter could be discovered in due course (e.g., by using interferometric techniques [52]). No doubt the passing from one degeneracy state to another would cause a release of huge amounts of energy previously stored in the form of the mass defect of the primitive particles, which could supply energy for gamma-ray bursts. These objects exhibit variability and multiple peaks in prompt emission on time scales from milliseconds to a few seconds [53] whose mechanism is not quite well understood. It is possible that a collapsing object would dispose of a great amount of its mass/energy before reaching the horizon, which might lead to the horizon oscillations [54] and observable peaks of emission corresponding to the structural phase transitions in the collapsing body. The detection of multiple neutrino outbursts from the supernova SN 1987A [55] also supports this phase transition conjecture.

This model leads to a self-consistent and verifiable framework, which might give an insight both into the nature of the cosmological singularity and the origin of the observed variety of elementary particles. It has inbuilt units of length, time and speed, fixing a scale against which this model can be compared with observations. Within its framework the dynamics of particles and sub-particles can be described in terms of well-established relativistic mechanics and Maxwell’s electrodynamics. On the other hand, this model uncovers the mechanisms behind some quantum phenomena (like particle spin, the Pauli exclusion principle, entanglement, virtual particles, etc.), which provides a link between the classical and quantum descriptions of physical reality. Although the characteristic length scale of this model is likely to be close to the Planck-length, one can, in principle, use this model to make calculations for much larger structures. An interesting area for further research would be exploring the phenomenological consequences of this framework on scales where more experimental tests could be conducted, e.g., on the scales of nuclear and atomic structures.

References

- [1] G. Lemaître, “L’univers en expansion”, *Ann. Soc. Sci. Bruxelles A* **53**, 51–85 (1933); R. C. Tolman, “Relativity, Thermodynamics and cosmology” (Oxford University Press, Clarendon Press, Oxford, 1934); F. Hoyle, G. Burbidge and J. Narlikar, “A different approach to cosmology” (Cambridge University Press, Cambridge, 2000).
- [2] P. J. Steinhardt and N. Turok, “A cyclic model of the universe”, *Science* **296**, 1436–1439 (2002); P. J. Steinhardt and N. Turok, “Cosmic evolution in a cyclic universe”, *Phys. Rev. D* **65**, 126003 (2002); P. J. Steinhardt and N. Turok, “Endless Universe: A New History of the Cosmos” (Doubleday Publ., N. Y., 2007);
- [3] J. A. Wheeler, “Geometrodynamics” (Academic Press, New York, 1962); D. Finkelstein and. C. W. Misner, “Some new conservation laws”, *Ann. Phys.* **6**, 230–243 (1959); J. Ambjorn, J. Jurkiewicz and R. Loll, “The universe from scratch”, *Contemp. Phys.* **47**, 103–117 (2006); H. I. Ringermacher and L. R. Mead, “Inducedmatter: Curved N-manifolds encapsulated in Riemann-flat N+1 dimensional space”, *J. Math. Phys.* **46**, 102501 (2005); D. Bohm, “Wholeness and the implicate order” (Rutledge, London, 1980).
- [4] R. Narayan, “Black holes in astrophysics”, *New J. Phys.* **7**, 199 (2005).
- [5] E. Kalemci et.al., “Multiwavelength observations of the galactic black hole transient 4U 1543-47 during outburst decay: state transitions and jet contribution”, *Astrophys. J.* **622**, 508–519 (2005).

- [6] M. S. Cropper et al., “Probable intermediate-mass black holes in NGC 4559: XMM-Newton spectral and timing constraints”, *Mon. Not. R. Astr. Soc.* **349**, 39–51 (2004).
- [7] M. J. Page et al., “Submillimetre evidence for the coeval formation of massive black holes and galaxy bulges”, *Science* **294**, 2516–2518 (2001); R. Bender et al., “HST STIS spectroscopy of the triple nucleus of M31: two nested disks in Keplerian rotation around a supermassive black hole”, *Astrophys. J.* **631**, 280–300 (2005).
- [8] G. Gamow, “The origin of elements and the separation of galaxies”, *Phys. Rev.* **74**, 505–506 (1948); A. A. Penzias and R. W. Wilson, “A measurement of excess antenna temperature at 4080 Mc/s”, *Astrophys. J.* **142**, 419–421 (1965); R. H. Dicke, P. J. E. Peebles, P. G. Roll and D. T. Wilkinson, “Cosmic black-body radiation”, *Astrophys. J.* **142**, 414–419 (1965).
- [9] I. Dymnikova, “The cosmological term as a source of mass”, *Class. Quantum Grav.* **19**, 725–739 (2002); I. Dymnikova and E. Galaktionov, “Vacuum dark fluid”, *Phys. Lett. B* **645**, 358–364 (2007).
- [10] A. Ashtekar, “Gravity and the quantum”, *New J. Phys.* **7**, 198 (2005).
- [11] Ya. B. Zeldovich, “Cosmological fluctuations produced near singularity”, *Mon. Not. R. Astr. Soc.* **192**, 663–667 (1980).
- [12] R. Ragazzoni, M. Turatto and W. Gaessler, “The lack of observational evidence for the quantum structure of spacetime at Planck scales”, *Astrophys. J.* **587**, L1–L4 (2003); R. Lieu and L. W. Hillman, “The phase coherence of light from extragalactic sources: Direct evidence against first-order Planck-scale fluctuations in time and space”, *Astrophys. J.* **585**, L77–L80 (2003).
- [13] I. G. Mitrofanov, “A constraint on canonical quantum gravity?” *Nature* **426**, 139 (2003).
- [14] S. Dado, A. Dar and A. De Rujula, “Implications of the large polarization measured in gamma-ray bursts”, in Proceed. of the Vulcano Workshop on Frontier Objects in Astrophysics, Vulcano, Italy, May 21–27, 2006 [arXiv: astro-ph/0701294].
- [15] D. Finkelstein, C. W. Misner, Some new conservation laws, *Ann. Phys.* **6**, 230–243 (1959).
- [16] C. F. E. Holzhey and F. Wilczek, “Black holes as elementary particles”, *Nucl. Phys. B* **380**, 447–477 (1992); A. Sen, “Extremal black holes and elementary string states”, *Modern. Phys. Lett. A* **10**, 2081 (1995); V. V. Flambaum and J. C. Berengut, “Atom made from charged elementary black hole”, *Phys. Rev. D* **63**, 084010 (2001); A. Ya. Burinski, “Super black hole as spinning particle”, in Proceed. of XXIV-th IHEP Workshop, ed. V.A.Petrov, 165–176 (IHEP Press, Protvino, 2001); Y. Ne’eman, “Primitive particle model”, *Phys. Lett. B* **82**, 69–70 (1979).
- [17] K. Gödel, “An example of new type of cosmological solutions of Einstein’s field equations of gravitation”, *Rev. Mod. Phys.* **21**, 447–450 (1949); S. W. Hawking and R. Penrose, “The singularities of gravitational collapse and cosmology”, *Proc. R. Soc. Lond. A* **314**, 529–548 (1970); F. J. Tipler, “Rotating cylinders and the possibility of global causality violation”, *Phys. Rev. D* **9**, 2203–2206 (1974); I. D. Novikov, “Physical properties of a time machine”, *Sov. Phys. Uspekhi* **32**, 282–283 (1989); J. Friedman et al, “Cauchy problem in spacetimes with closed timelike curves”, *Phys. Rev. D* **42**, 1915–1930 (1990); V. E. Hubeny, M. Rangamani and S. F. Ross, “Causally pathological space-times are physically relevant”, *Int. J. Mod. Phys. D* **14**, 2227–2231 (2005).
- [18] R. de Ritis, M. Lavorgna, G. Platania and C. Stornaiolo, “Spin fluid in Einstein-Cartan theory: A variational principle and an extension of the velocity potential representation”, *Phys. Rev. D* **28**, 713–717 (1983); B. M. Barbashov and A. B. Pestov, “Antisymmetric tensor fields and the Weyl gauge theory”, *Theor. Math. Phys.* **113**, 1299–1308 (1997); A. Dimakis and F. Müller-Hoissen, “Differential geometry of group lattices”, *J. Math. Phys.* **44**, 1781–1821 (2003).
- [19] V. D. Dzhunushaliev, “Spherically-symmetric solution for torsion and the Dirac equation in 5D spacetime”, *Intern. J. Mod. Phys. D* **7**, 909–915 (1998); M. Alimohammadi, “Some correlators of $SU(3)_3$ WZW models on higher-genus Riemann surfaces”, *Mod. Phys. Lett. A* **9**, 381–398 (1994).
- [20] R. Jackiw, V. P. Nair and S.-Y. Pi , “Chern-Simons reduction and non-Abelian fluid mechanics”, *Phys. Rev. D* **62**, 085018 (2000); B. Byストovic, R. Jackiw, H. Li, V. P. Nair and S.-Y. Pi, “Non-Abelian fluid dynamics in Lagrangian formulation”, *Phys. Rev. D* **67**, 025013 (2003); J. Dai and V. P. Nair, “Color Skyrmions in the quark-gluon plasma”, *Phys. Rev. D* **74**, 085014 (2006).
- [21] O. Tornkvist and E. Schroder, “Vortex dynamics in dissipative systems”, *Phys. Rev. Lett.* **78**, 1908–1911 (1997); J. R. Grant and J. S. Marshall, “Inviscid interaction of vortex rings: approach to singularity?”, *Third Intern. Workshop on Vortex Flows and Related Numerical Methods*, ESAIM: Proceed. **7**, 183–194 (1999).

- [22] O. V. Baburova, B. N. Frolov, A. S. Vshivtsev and V. P. Myasnikov, “A model of perfect fluid with spin and nonabelian color charge”, *Phys. Dokl.* **42**, 611–614 (1997); R. T. Hammond, “Torsion power”, *Gen. Rel. Grav.* **29**, 727–731 (1997).
- [23] E. F. Suisso, J. P. B. C. de Melo and T. Frederico, “Relativistic dynamics of Qqq systems”, *Phys. Rev. D* **65**, 094009 (2002).
- [24] S. Ansoldi, P. Nicolini, A. Smailagic and E. Spalucci, “Non-commutative geometry inspired charged black holes”, *Phys. Lett. B* **645**, 261–266 (2007).
- [25] O. Osenda, P. Serra and F. A. Tamarit, “Non-equilibrium properties of small Lennard-Jones clusters”, *Physica D* **168–169**, 336–340 (2002).
- [26] S. Wiggins, “Global Bifurcations and Dynamical Chaos” (Springer-Verlag, Berlin, 1988); L. Carlson and W. C. Schieve, “Chaos and quantum fluctuations in the squeezed double-well potential”, *Phys. Rev. A* **40**, 1127–1129 (1989).
- [27] M. Kleman, Lines and Walls, Wiley and Sons, Chichester, 1983.
- [28] A. Pikovsky, M. Rosenblum and J. Kurths, “Synchronization: a Universal Concept in Nonlinear Sciences” (Cambridge Univ. press, Cambridge, 2001).
- [29] V. N. Yershov, “Equilibrium configurations of tripolar charges”, *Few-Body Syst.* **37**, 79–106 (2005).
- [30] V. Silveira and A. Zee, “Preons with exceptional hyperforce”, *Phys. Lett. B* **157**, 191–194 (1985).
- [31] V. N. Yershov, “Quantum properties of a cyclic structure based on tripolar fields”, *Physica D* **226**, 136–143 (2007).
- [32] H. G. Dehmelt, “Experiments with an isolated subatomic particle at rest”, *Nobel Lectures, Physics 1981–1990*, Ed. T. Frängsmyr and G. Ekspang, 583–595 (World Scientific Publ., Singapore, 1993).
- [33] G. Dissertori, “LHC expectations (machine, detectors and physics)”, Proceed. of the International Europhysics Conference on High Energy Physics (HEP-EPS 2005), Lisbon, Portugal, 21-27 Jul 2005, [arXiv: hep-ex/0512007]; K. Desch, “LHC physics – what can be done in the first years”, *Acta Phys. Polonica B* **36**, 3343–3353 (2005); D. Treile, “The experimental challenges of LHC”, *J. of Phys.: Conf. Series* **53**, 117–162 (2006).
- [34] D. Stump, “Inclusive jet production, parton distributions, and the search for new physics”, *JHEP* **10**, 046 (2003); G. Domokos and S. Kovács-Domokos, “Some signals of compositeness of quarks and leptons”, *Phys. Lett. B* **266**, 87–91 (1991).
- [35] D. Treille, “The experimental challenges of LHC”, *J. Phys. Conf. Ser.* **53**, 117–162 (2006); P. Miné, “Exotica at LHC”, *EPJdirect C* **4**, Suppl. 1, 18 (2002).
- [36] H. Senju, “Preon model and exotic events”, *Progr. Theor. Phys.* **74**, 413–417 (1985).
- [37] R. Harnik, G. D. Kribs and G. Perez, “A universe without weak interaction”, *Phys. Rev. D* **74**, 035006 (2006).
- [38] F. Bloch, “Bemerkung zur Elektronentheorie des Ferromagnetismus und der electrische Leitfähigkeit”, *Z. Phys.* **57**, 545–555 (1929).
- [39] M. M. Fogler and E. Pivovarov, “Spin exchange in quantum rings and wires in the Wigner-crystal limit”, *J. Phys.: Condens. Matter* **18**, I.7–I.13 (2006).
- [40] P. I. Jain and G. Singh, “Search for new particles decaying into electron pairs of mass below 100 MeV/c²”, *J. Phys. G: Nucl. Part. Phys.* **34**, 129–138 (2007).
- [41] L. L. Cowie and A. Songalia, “Astrophysical limits on the evolution of dimensionless physical constants over cosmological time”, *Astrophys. J.* **453**, 596–598 (1995); A. Y. Potekhin et al., “Testing cosmological variability of the proton-to-electron mass ratio using the spectrum of PKS 0528-250”, *Astrophys. J.* **505**, 523 (1998); M. Levshakov, S. Dessauges-Zavadsky, S. D’Orioco and P. Molaro, “A new constraint on cosmological variability of the proton-to-electron mass ratio”, *Mon. Not. R. Astron. Soc.* **333**, 373–377 (2002).
- [42] M. M. Ćirković, “Is the universe really that simple?”, *Found. Phys.* **32**, 1141–1157 (2002); Ya. B. Zeldovich, “A hypothesis, unifying the structure and the entropy of the universe”, *Mon. Not. R. Astr. Soc.*, **160**, 1–3 (1972).

- [43] W. P. Thurston and J. Weeks, “The mathematics of three-dimensional manifolds”, *Sci. Am.* **251**, 108–113 (1984); M. Anderson, “Curvature estimates for minimal surfaces in 3-manifolds”, *Ann. Scient. Ecole Norm. Sup.* **18**, 89–105 (1985); W. P. Thurston, “Three-Dimensional Geometry and Topology”, Vol. 1, 25–18 (Princeton Univ. Press, Princeton NJ, 1997).
- [44] D. Jakobson, N. Nadirashvili and I. Polterovich, “Extremal metric for the first eigenvalue on a Klein bottle”, *Canad. J. Math.* **58**, 381–400 (2006).
- [45] D. N. Spergel et al, “First year Wilkinson Microwave Anisotropy Probe (WMAP) observations: determination of cosmological parameters”, *Astrophys. J. Suppl.* **148**, 175–194 (2003).
- [46] J. Anandan, Global topology and local violation of discrete symmetries, *Phys. Rev. Lett.* **81** 1363–1366 (1998); F. R. Klinkhamer, A CPT anomaly, *Nucl. Phys.* **B578**, 277–289 (2000); F. R. Klinkhamer and J. Schimmel, CPT anomaly: a rigorous result in four dimensions, *Nucl. Phys.* **B639**, 241 (2002); F. R. Klinkhamer and C. Rupp, Spacetime foam, CPT anomaly and photon propagation, *Phys. Rev.* **D70**, 045020 (2004).
- [47] A. Albrecht, J. Magueijo, A time varying speed of light as a solution to cosmological puzzles, *Phys. Rev.* **D59**, 043516 (1999); J. D. Barrow, “Cosmologies with varying light-speed” [arXiv: astro-ph/9811022]; M. Szydlowski and A. Krawiec A., “Dynamical system approach to cosmological models with varying speed of light” [arXiv: gr-qc/0212068]; G. Ellis, R. Maartens, “The emergent universe: inflationary cosmology with no singularity and no quantum gravity era” [arXiv: gr-qc/0211082]; J. C. Niemeyer, “Varying speed of light cosmology from a stringy short distance cutoff”, *Phys. Rev. D* **65**, 083505 (2002); J. Magueijo, “Stars and black holes in varying speed of light theories”, *Phys. Rev. D* **63**, 043502 (2001).
- [48] J. Magueijo, “New varying speed of light theories”, *Rept. Prog. Phys.* **66**, 2025–2068 (2003).
- [49] S. Chakraborty, “Varying-speed-of-light theory with a variable cosmological term”, *Nuovo Cimento B* **117**, 189–195 (2002).
- [50] A. B. Balakin, D. Pavón, D. J. Schwarz and W. Zundahl, “Curvature force and dark energy”, *New J. Phys.* **5**, 85 (2003).
- [51] T. Asselmeyer-Maluga and H. Rosé, “Calculation of the cosmological constant by unifying matter and dark energy” [arXiv: gr-qc/0609004]; F. P. Devecchi and M. L. Froenlich, “3D gravity and nonlinear cosmology”, *Mod. Phys. Lett. A* **21**, 445–450 (2006).
- [52] F. Sandin and J. Hansson, Observational legacy of preon stars: probing new physics beyond CERN LHC, *Phys. Rev. D* (to be published) [arXiv: astro-ph/0701768].
- [53] F. Frontera et al., “The prompt emission of GRB 990712 with BeppoSAX: Evidence of a transient X-ray emission feature”, *Astroph. J.* **550**, L47–L51 (2001).
- [54] P. Anninos et al., “Dynamics of apparent and event horizons”, *Phys. Rev. Lett.* **75**, 630–633 (1995); I. A. Urusovskii, “Supplement to Harmonic solutions to Einstein equations”, *Russian Phys. J.* **22**, 1001–1002 (1979).
- [55] I. Goldman, Y. Aharonov, G. Alexander and S. Nussinov, “Implications of the supernova SN 1987A neutrino signals”, *Phys. Rev. Lett.* **60**, 1789–1792 (1988); D. N. Voskresensky, A. V. Senatorov, B. Kaempfer and H. J. Haubold, “Possible explanation of the second neutrino burst from SN 1987A”, *Astroph. and Space Sci.* **138**, 421–424 (1987); M. E. Gertsenshtein, “About neutrino signals from SN 1987A”, *Il Nuovo Cim. C* **12**, 835–840 (1989); D. Saha and G. Chattopadhyay, “Periodicities of the neutrino burst from supernova 1987A”, *Astrophys. and Space Sci.* **178**, 209–215 (1991).